Geometrical and Statistical Visual Inspection of Imprinted Tablets

Marko Bukovec, Žiga Špiclin, Franjo Pernuš and Boštjan Likar
University of Ljubljana,
Faculty of Electrical Engineering, Tržaška 25, 1000 Ljubljana, Slovenia
E-mail: {marko.bukovec, ziga.spiclin, franjo.pernus, bostjan.likar}@fe.uni-lj.si

Abstract

In this paper we address automated visual inspection of tablets that may, in contrast to manual tablet sorting, provide objective and reproducible tablet quality assurance. Visual inspection of the ever–increasing numbers of the produced imprinted tablets, regulatory enforced for unambiguous identification of active ingredients and dosage strength of each tablet, is especially demanding. The problem becomes more tractable by incorporating some a priori knowledge of the imprint shape and/or appearance. For this purpose, we consider two alternatives, the so-called geometrical and statistical image analysis methods. The geometrical method, incorporating geometrical a priori knowledge of the imprint shape, enables specific inspection of imprinted and non-imprinted tablet surface, while the statistical method exploits a priori knowledge of tablet surface appearance, derived from a training image database. The two methods were evaluated on a large tablet image database, consisting of 3445 images of four types of imprinted tablets, with and without typical production defects. A "gold standard" for testing the performances of the two inspection methods was established by manually classifying the tablets. The results, obtained by ROC analysis, indicated that statistical method yields better defect detection sensitivity and specificity and is thus more suitable for automatic visual inspection of imprinted tablets.

1. Introduction

Nowadays, pharmaceutical companies produce a vast amount of different tablets worldwide. Tablet features, like shape, size, color, imprints, etc., must enable both professionals and consumers to unambiguously identify the tablet and its dosage strength. This regulatory enforced requirement poses at least two challenging and interwinded problems to the pharmaceutical companies. First, the manufacturing processes must be updated or remodeled so as to produce tablets of different size, shape, color, texture, and/or imprints [1]. At the same time, the companies are also required to maintain or even improve the quality of the produced tablets, which is the second and contradicting problem, especially when producing tablets of complex shapes and/or imprints as these are far more difficult to produce. Consequently, various visual defects may emerge from the demanding manufacturing process, reducing the overall visual quality of the produced tablets. The problem is especially severe when affecting the visibility and/or readability of tablet imprints. This may result in hazardous mix-ups among various types of tablets and thereby possibly endanger human life. In this respect, visual tablet inspection is of the utmost importance for assuring the required quality of different tablets.

Visual quality inspection of tablets is nowadays often performed manually by various statistical sampling schemes. Such procedures only estimate, at a certain confidence level, the overall quality of a given batch of tablets and can thus not assure the required quality of each tablet. To reach this goal, manual or automated visual inspection of each tablet from all sides is required but since manual visual inspection is subjective, unreliable, tedious and even harmful to the operators, only automated visual inspection becomes feasible nowadays for assuring the required quality of huge tablet batches.

Automated visual quality inspection of tablets requires a sophisticated machine vision system, capable of fast tablet manipulation and illumination, image acquisition, and processing, estimation of tablet features/defects and corresponding classification and sorting. The key for reliable tablet inspection and sorting is efficient estimation of visual tablet features by means of automated tablet image analysis. Feature estimation is especially demanding when tablets with imprints are inspected as imprint areas may have significantly different visual properties than the rest of the tablet surface. The problem becomes more tractable, also for the various types of tablets, if some a priori knowledge of the imprint shape and/or appearance is incorporated into the tablet feature estimation step. In this case, imprinted and non-imprinted tablet surfaces can be analyzed differently and specifically for each tablet type.

In this paper, we consider two alternative image analysis methods for tablet specific estimation of visual features of imprinted tablets, one incorporating a priori knowledge of the imprint shape, the other of the whole tablet surface appearance. The two methods were evaluated on a large image database of imprinted tablets, with and without typical production defects. The sensitivities and specificities for detecting various defects on imprinted tablets were assessed by the ROC analysis.

2. Methods

In this section, the so-called geometrical and statistical image analysis methods are presented. The methods operate on tablet images and extract different visual features, estimating tablet surface quality. Features are derived from different column vector representations $\mathbf{x}$ of tablet image $\mathbf{I}$, which were in a form of image intensities $\mathbf{i}$, absolute gradients $\mathbf{g}$ and gradient components $\mathbf{c}=[\mathbf{c}_x^{\mathrm{T}}, \mathbf{c}_y^{\mathrm{T}}]^{\mathrm{T}}$ in x and in y directions.

2.1. Geometrical method

The geometrical method incorporates a priori knowledge of the imprint shape in a geometrical form so that the imprint region can be analyzed separately, i.e. independently of the rest of the tablet surface. It is assumed that partitioning of the tablet surface into two non-overlapping constituent regions, each with specific visual properties, can increase the sensitivity and specificity of the extracted visual features/defects in both tablet regions.

A priori knowledge of the imprint shape is obtained from the imprint design, superimposed on the tablet image. The imprint is represented by a skeleton, defining local imprint direction and a binary imprint template of a selected thickness. The so-called geometrical features are computed separately for the imprint and non-imprint regions of the tablet surface.

Two geometrical features are computed as maximal G_1 and minimal G_2 difference between the original $\mathbf{i}$ and filtered $\mathbf{i}^*$ image intensities in a given tablet region Ω:

$$G_1 = \max_{\Omega} (\mathbf{i} - \mathbf{i}^*), \quad G_2 = \min_{\Omega} (\mathbf{i} - \mathbf{i}^*) \qquad (1)$$

Another two geometrical features are defined as maximal G_3 absolute gradient $\mathbf{g}$ and maximal G_4 filtered absolute gradient $\mathbf{g}^*$:

$$G_3 = \max_{\Omega} \mathbf{g}, \quad G_4 = \max_{\Omega} \mathbf{g}^* \qquad (2)$$

The last geometrical feature is derived from the component gradient $\mathbf{c}$ in the imprint region as a maximal G_5 scalar product between gradient component $\mathbf{c}$ and normalized local imprint direction vector $\mathbf{s}$, defined by the imprint skeleton:

$$G_5 = \max_{\Omega} \left\| \mathbf{c}_p \cdot \mathbf{s}_p \right\| \cdot \left\| \mathbf{s}_p \right\|^{-1} \qquad (3)$$

where $\mathbf{c}_p$ and $\mathbf{s}_p$ represent the gradient component vector $\mathbf{c}$ and normalized local imprint direction vector $\mathbf{s}$ at each image point $p(x,y)$:

$$\mathbf{c}_p = [\, c_x \;\; c_y \,]^T \quad \text{and} \quad \mathbf{s}_p = [\, s_x \;\; s_y \,]^T \qquad (4)$$

2.2. Statistical method

The statistical method exploits the statistical a priori knowledge of the entire tablet surface appearance, derived from a training image database. In this way, not only the imprint and non-imprint tablet regions but also each image element (pixel) is inherently analyzed distinctively and specifically for each tablet type.

Principal component analysis [2, 3] is used to statistically model tablet surface appearance by a linear model:

$$\mathbf{x} = \bar{\mathbf{x}} + \mathbf{A}\mathbf{p} \qquad (5)$$

A set of N aligned training images $\mathbf{I}_1 \ldots \mathbf{I}_N$ are converted to column vector representations $\mathbf{x}_1 \ldots \mathbf{x}_N$ and the corresponding average column vector $\bar{\mathbf{x}}$ and covariance matrix Θ are computed:

$$\Theta = E(\,(\mathbf{x} - \bar{\mathbf{x}})(\mathbf{x} - \bar{\mathbf{x}})^T\,) \qquad (6)$$

Next, the eigenvalues and corresponding eigenvectors of the covariance matrix Θ are obtained by singular value decomposition [4]. The eigenvectors of the largest eigenvalues represent the most significant modes of variation of tablet surface appearance over a set of training images.

Tablet surface appearance can be thus approximated by only the first t most significant eigenvectors:

$$\mathbf{x} \approx \tilde{\mathbf{x}} = \bar{\mathbf{x}} + \mathbf{A}_t \mathbf{p}_t \qquad (7)$$

where $\tilde{\mathbf{x}}$ denotes an approximation of $\mathbf{x}$, $\mathbf{A}_t$ the first t eigenvectors of Θ and $\boldsymbol{p}_t$ a vector of appearance approximation parameters, i.e. projections of $(\mathbf{x} - \bar{\mathbf{x}})$ to the corresponding t eigenvectors. In this way, a compact statistical model, representing a priori knowledge of tablet surface appearance, can be obtained for any tablet image representation $\mathbf{x}$. In our case, we have used image intensities $\mathbf{i}$, absolute gradients $\mathbf{g}$ and gradient components $\mathbf{c}$ of the tablet images and derived the corresponding statistical models of their appearances. The obtained statistical models are used to derive various so-called statistical features of tablet images aligned to the statistical models.

The first statistical feature is derived as a maximal absolute difference S_1 between the tablet image intensity representation $\mathbf{i}$ and corresponding statistical model $\tilde{\mathbf{i}}$, over the entire tablet surface domain Ω:

$$S_1 = \max_{\Omega} \left| \mathbf{i} - \tilde{\mathbf{i}} \right| \qquad (8)$$

Another statistical feature is obtained as the maximal absolute difference S_2 between the tablet image gradient representation $\mathbf{g}$ and corresponding statistical model $\tilde{\mathbf{g}}$, over the entire tablet surface domain Ω:

$$S_2 = \max_{\Omega} \left| \mathbf{g} - \tilde{\mathbf{g}} \right| \qquad (9)$$

The last three statistical features are obtained by comparing gradient components $\mathbf{c}$ of the analyzed tablet images and corresponding statistical model $\tilde{\mathbf{c}}$. The gradient components are compared by a vector difference S_3, vector product S_4, and normalized vector product S_5:

$$S_3 = \max_{\Omega} \left\| \mathbf{c}_p - \tilde{\mathbf{c}}_p \right\| \qquad (10)$$

$$S_4 = \max_{\Omega} \left\| \mathbf{c}_p \times \tilde{\mathbf{c}}_p \right\| \qquad (11)$$

$$S_5 = \max_{\Omega} \left\| \mathbf{c}_p \times \tilde{\mathbf{c}}_p \right\| \cdot \left\| \tilde{\mathbf{c}}_p \right\|^{-1} \qquad (12)$$

where $\mathbf{c}_p$ and $\tilde{\mathbf{c}}_p$ respectively denote the values of gradient component and corresponding statistical model at each image point $p(x,y)$:

$$\mathbf{c}_p = [\, c_x \;\; c_y \,]^T \quad \text{and} \quad \tilde{\mathbf{c}}_p = [\, \tilde{c}_x \;\; \tilde{c}_y \,]^T \qquad (13)$$

3. Experiments and results

In this section, the implementation details, the experimental tablet image database with the "gold standard", and the evaluation methodology are presented first. Next, the defect detection results obtained by the five geometrical and five statistical features are given.

3.1. Implementation details

Filtered image intensities $\mathbf{i}^*$ and gradient components $\mathbf{c}$ were obtained from the original intensities $\mathbf{i}$ using an uniform filter with 5x5 kernel, while a larger 20x20 kernel was used for filtering the absolute gradients $\mathbf{g}^*$. The statistical models of appearances of each tablet type were derived from 80 training images and approximated by the first three eigenvectors ($t=3$).

3.2. Image database with "gold standard"

The experimental image database consisted of 3445 images of four types of imprinted tablets taken from production line in sets of 830, 1208, 821 and 586 tablets, with and without typical defects. A "gold standard" for visual inspection of defects was established by carefully manually classifying the tablets among the defective and non-defective ones. The tablets were classified into five defect categories, named: dot (D_1), spot (D_2), emboss (D_3), deboss (D_4) and crack (D_5), as illustrated by the examples in Figure 1.
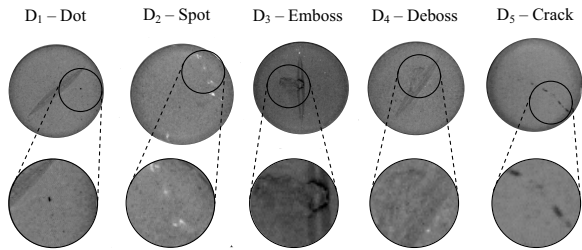
Figure 1. Tablets (top) with zoomed defects (bottom).

3.3. Evaluation methodology

The specificities and corresponding sensitivities of geometrical (G_1–G_5) and statistical (S_1–S_5) features for each defect category in each tablet set were obtained by the Receiver Operating Characteristics (ROC) analysis [5]. The ROC curve relates the tradeoffs between the true positive (TPR) and the corresponding false positive (FPR) defect detection rate of each feature. The TPR=TP/P is a ratio between the number of correctly detected tablets with defects (TP) and all defective (P) tablets, while the FPR=FP/N represents a ratio between the number of incorrectly detected non-defective tablets (FP) and all non-defective (N) tablets. TPR is a measure of sensitivity,

while 1-FPR is a measure of defect detection specificity. ROC curve is insensitive to the ratio between the number of defective and non-defective "gold standard" samples used for evaluation.

For the sake of transparency, two additional evaluation criteria, TPR_{FPR} and AUC_{FPR}, were derived from the ROC curves of the geometrical and statistical features. The TPR_{FPR} is the value of TPR at a given FPR and therefore represents the ratio of correctly detected tablets with defects at a given ratio of the incorrectly detected tablets. On the other hand, the AUC_{FPR} is the area under the ROC curve in an interval from 0 to a given FPR, normalized by the interval length. AUC_{FPR} thus estimates the average defect detection performance over the practically acceptable interval of the FPR for a given application.

In our case, we have selected the acceptable FPR of 0.1 and therefore computed the corresponding $TPR_{0.1}$ and $AUC_{0.1}$ from the ROC curves of all geometrical and statistical features and all defect categories. To assess both defect-specific and general defect detection performances of individual features, the features were separately evaluated for the detection of individual defect categories.

3.4. Results

The results of the defect detection by the geometrical and statistical features are shown in Tables 1-3. Tables 1 and 2 show the obtained values of $TPR_{0.1}$ and $AUC_{0.1}$ for all features and defect categories (D_1–D_5) of the first two tablet sets, while in Table 3 only the results for all defect categories (D_{ALL}) from the third and fourth tablet sets are given. In all three tables, the best $TPR_{0.1}$ and $AUC_{0.1}$ values are marked in bold so that the best features can easily be identified.

The obtained results indicate that the statistical feature S_3 performs the best for the detection of defects in all four sets of tablets. Statistical features S_2 and S_5 also performed

Table 1. The $TPR_{0.1}$ and $AUC_{0.1}$ values for all features and all defects in the first set of 830 tablet images.

Set 1	D_1		D_2		D_3		D_4		D_5		D_{ALL}	
Feature	$TPR_{0.1}$	$AUC_{0.1}$	$TPR_{0.1}$	$AUC_{0.1}$	$TPR_{0.1}$	$AUC_{0.1}$	$TPR_{0.1}$	$AUC_{0.1}$	$TPR_{0.1}$	$AUC_{0.1}$	$TPR_{0.1}$	$AUC_{0.1}$
G_1	0.38	0.32	0.57	0.45	0.55	0.53	0.33	0.24	0.75	0.57	0.41	0.30
G_2	0.70	0.55	0.61	0.55	0.62	0.52	0.37	0.24	0.55	0.44	0.47	0.34
G_3	0.83	0.73	0.83	0.72	0.58	0.54	0.51	0.44	**1.00**	0.87	0.63	0.56
G_4	0.90	0.84	**1.00**	**0.98**	0.64	0.57	0.73	0.68	**1.00**	**1.00**	0.80	0.74
G_5	0.52	0.50	0.44	0.42	0.59	0.53	0.85	0.83	0.05	0.03	0.61	0.59
S_1	0.94	0.82	0.88	0.74	**1.00**	0.92	**1.00**	0.85	0.95	0.78	0.96	0.82
S_2	**1.00**	0.91	**1.00**	0.95	**1.00**	0.96	**1.00**	0.92	**1.00**	0.99	**1.00**	0.92
S_3	**1.00**	**0.97**	**1.00**	0.97	**1.00**	**1.00**	**1.00**	**1.00**	**1.00**	0.99	**1.00**	**0.98**
S_4	0.64	0.57	0.47	0.39	**1.00**	0.65	0.98	0.91	0.55	0.50	0.75	0.67
S_5	**1.00**	0.94	**1.00**	0.96	**1.00**	0.93	**1.00**	0.95	**1.00**	0.99	**1.00**	0.94

Table 2. The $TPR_{0.1}$ and $AUC_{0.1}$ values for all features and all defects in the second set of 1208 tablet images.

Set 2	D_1		D_2		D_3		D_4		D_5		D_{ALL}	
Feature	$TPR_{0.1}$	$AUC_{0.1}$	$TPR_{0.1}$	$AUC_{0.1}$	$TPR_{0.1}$	$AUC_{0.1}$	$TPR_{0.1}$	$AUC_{0.1}$	$TPR_{0.1}$	$AUC_{0.1}$	$TPR_{0.1}$	$AUC_{0.1}$
G_1	0.44	0.30	0.60	0.54	0.65	0.53	0.53	0.45	1.00	1.00	0.40	0.29
G_2	0.53	0.39	0.58	0.43	**1.00**	0.73	0.44	0.29	1.00	1.00	0.46	0.32
G_3	0.69	0.56	0.89	0.73	**1.00**	0.88	0.66	0.50	1.00	1.00	0.64	0.51
G_4	0.64	0.47	0.91	0.89	**1.00**	**1.00**	0.79	0.71	1.00	1.00	0.66	0.53
G_5	0.37	0.29	0.60	0.58	**1.00**	**1.00**	0.74	0.71	1.00	1.00	0.45	0.40
S_1	0.74	0.65	0.91	0.86	**1.00**	0.97	0.91	0.85	1.00	1.00	0.77	0.68
S_2	**0.87**	0.75	**0.95**	**0.91**	**1.00**	**1.00**	**1.00**	0.90	1.00	1.00	**0.91**	0.78
S_3	0.85	**0.76**	**0.95**	**0.91**	**1.00**	**1.00**	**1.00**	**0.98**	1.00	1.00	0.90	**0.82**
S_4	0.38	0.24	0.58	0.46	**1.00**	0.99	0.75	0.52	1.00	1.00	0.49	0.32
S_5	0.84	**0.76**	0.94	**0.91**	**1.00**	**1.00**	**1.00**	0.93	1.00	1.00	0.88	0.80

Table 3. The $TPR_{0.1}$ and $AUC_{0.1}$ values for all features in the third and fourth set of 821 and 586 tablet images, respectively.

Feature	Set 3 - D_{ALL}		Set 4 - D_{ALL}	
	$TPR_{0.1}$	$AUC_{0.1}$	$TPR_{0.1}$	$AUC_{0.1}$
G_1	0.40	0.22	0.23	0.16
G_2	0.04	0.02	0.25	0.12
G_3	0.45	0.23	0.59	0.42
G_4	0.94	0.78	0.41	0.36
G_5	0.36	0.32	0.27	0.20
S_1	0.83	0.66	0.74	0.46
S_2	0.92	0.77	**0.91**	0.78
S_3	0.93	**0.83**	0.90	**0.80**
S_4	0.48	0.34	0.26	0.23
S_5	**0.96**	0.81	0.85	0.77

well on all sets of tablets. On the other hand, geometrical features yielded much lower true positive detection rates on all defects, with an exception of feature G_4. However, a comparison of the best geometrical G_4 to the best statistical feature S_3, given also by the ROC curves for the first tablet set in Figure 2, indicate that the statistical feature S_3 performs much better. Moreover, in the first tablet set, the best geometrical feature yielded a $TPR_{0.1}$ value of 0.80, while three statistical features performed perfectly with the $TPR_{0.1}$ values of 1. In the second set of images, the best $TPR_{0.1}$ values of 0.66 and 0.91 were obtained by the best geometrical and best statistical features, respectively. In sets three and four, the best geometrical $TPR_{0.1}$ values were 0.94 and 0.59, while the best statistical features yielded $TPR_{0.1}$ values of 0.96 and 0.91, respectively.
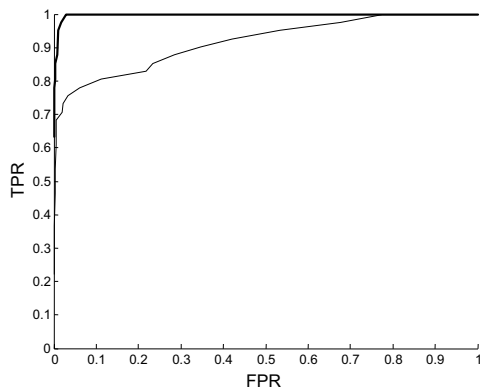
Figure 2. ROC curves of geometrical G_4 (thin) and statistical feature S_3 (thick) for the first tablet set.

4. Discussion and conclusion

Two alternative image analysis methods, based on geometrical and statistical a priori knowledge, were introduced and compared for visual inspection of typical production defects on imprinted tablets. The methods were tested on a large representative image database of four types of tablets. The obtained results demonstrated that both methods perform adequately, while the statistical method yielded better sensitivity and specificity on all types of tablets and defects. In both methods, the features based on image gradients outperformed the features based on image intensities. Altogether, the statistical features based on component gradients performed the best, which was to be expected since component gradients are gener-

ally more descriptive than absolute gradients or intensities.

Other important practical issues are the reliability of the inspection phase and simplicity of the training phase, which is required by both methods before inspecting a new type of products. Namely, the geometrical method requires a construction of a skeleton and corresponding binary model of an imprint, which can be obtained automatically from the tablet design or manually on a selected tablet image. On the other hand, the statistical method requires construction of statistical models of appearances that can be derived automatically from the aligned training images of each new tablet type. Therefore, considering the training phase, the statistical method seems more automated and thereby also more practical but requires reliable rigid registration of tablet images. Image registration also plays an important role in the inspection phase of both methods. Namely, the geometrical and statistical methods require automatic rigid registration of the inspected tablet image to the corresponding geometrical and statistical models, respectively. Nevertheless, rigid registration is a well established image analysis field [6].

The high specificity (low FPR) of the visual quality inspection has huge practical and economical benefits as less non-defective products are detected as defective and thereby mistakenly discarded. On the other hand, the increased sensitivity (high TPR) is of the utmost importance for the final quality of a given tablet batch. In terms of specificity and sensitivity, statistical method and especially component gradient features seem feasible for visual quality inspection of different types of tablets. Nevertheless, the presented image analysis methods are quite general and promising tools for automated visual inspection of not only tablets but also capsules or other solid oral dosage forms.

Acknowledgments

References

[1] FDA, Code of Federal Regulations (21CFR206), Imprinting of solid oral dosage form drug products for human use: http://www.accessdata.fda.gov/scripts/cdrh/cfdocs/cfcfr/CFRSearch.cfm?CFRPart=206

[2] T. F. Cootes, G. J. Edwards, and C. J. Taylor, "Active appearance models," *IEEE Transactions On Pattern Analysis And Machine Intelligence*, vol. 23, pp. 681-685, 2001.

[3] B. Moghaddam and A. Pentland, "Probabilistic, View-Based, and Modular Models for Human Face Recognition," in *Handbook of Image and Video Processing*, A. Bovik, Ed.: Academic Press, 2000, pp. 837-852.

[4] W. H. Press, S. A. Teukolsky, W. T. Vetterling, and B. P. Flannery, "Numerical recipes in C: The art of scientific computing," Cambridge University Press, 1992, pp. 59-70, 408-412.

[5] T. Fawcett, "An introduction to ROC analysis," *Pattern Recognition Letters*, vol. 27, pp. 861-874, 2006.

[6] B. Zitova and J. Flusser, "Image registration methods: A survey," *Image and Vision Computing*, vol. 21, pp. 977-1000, 2003.